Bis(bipyridine)-phenanthroline double-stranded helicates of the d^{10} metals: zinc(II), silver(I) and copper(I) helicates†

Moshe Greenwald, Dana Wessely, Israel Goldberg and Yoram Cohen*

School of Chemistry, The Sackler Faculty of Exact Sciences, Tel Aviv University, Ramat Aviv,
Tel Aviv 69978, Israel. Fax: +972-3-6409293; E-mail: ycohen@ccsg.tau.ac.il

Received (in Montpellier, France) 5th November 1998, Accepted 21st December 1998

The new ligand 2,9-bis[(6-methyl-2,2′-bipyridin-6′-yl)methyleneoxymethylen-yl]-1,10-phenanthroline (**1**) was prepared and was shown to self-assemble into double-stranded helicates upon reaction with Cu^+, Ag^+ and Zn^{2+}, thus affording the first trinuclear double-stranded zinc helicate. The $[(\mathbf{1})_2M_3]^{3n+}$ [$M = Cu^+ (n = 1)$, $Ag^+ (n = 1)$ or $Zn^{2+} (n = 2)$] helicates were characterized by 1D, 2D and diffusion NMR. FAB mass spectrometry corroborated the structure of the silver and the copper helicates and $[(\mathbf{1})_2Cu_3]^{3+}$ was characterized by X-ray crystallography. The detailed assignments of the ^1H NMR spectra of these helicates have shown that H-10 absorbs at a much higher field when compared to the other protons of these complexes. This high-field shift is a unique characteristic of the helicates of **1** and is not found in structurally related helicates. The NMR spectra of these helicates, at room temperature, are consistent with an average solution structure having a D_2 symmetry. Variable-temperature ^1H NMR (VT-NMR) reveals that the silver helicate of **1** is much more labile than its copper helicate. From the VT-NMR spectra it seems that two, nearly separate, stages are observed in the dissociation process of $[(\mathbf{1})_2Ag_3]^{3+}$. The activation energy of the first process for $[(\mathbf{1})_2Ag_3]^{3+}$ in DMSO-d_6 was found to be 16.6 ± 0.2 kcal mol^{-1}. As expected, the energy barriers for the respective copper helicate are even higher. The crystal structure of $[(\mathbf{1})_2Cu_3]^{3+}$ shows that the total length and the pitch length are ≈17 and 12 Å, respectively.

The preparation of synthetic helicates, by self-assembly processes,[1,2] has attracted considerable attention in recent years.[3–7] Ligands composed of 2,2′-bipyridine and 2,2′:6′,2″-terpyridine were shown to form double-stranded helicates using tetrahedral and octahedral cations, respectively.[3–7] Bidentate and tridentate ligands were also shown to self-assemble into stable triple-stranded helicates.[6,7] Previously, many of the organic ligands used in the preparation of helicates were composed of repetitive molecular units. However, more recently heterohelicates made of ligands that contain different coordination sites have been prepared.[8,9] In addition, mixed helicates in which the coordination sites discriminate between metal cations according to their electronic and geometric preferences have been prepared.[10] For example, quinquepyridine, which is a simple oligopyridine, was shown to act as a superposition of a bi- and a tridentate ligand, thus forming a heteronuclear helicate.[10a] Another family of heteronuclear helicates was prepared by Piguet who has demonstrated the potential of such complexes as molecular lanthanide probes and sensors.[10b] Shanzer and colleagues' triple helix, which contains two different coordination sites, was shown to operate as a molecular switch.[11] Another example is the stabilization of the pentacoordinate Cu^{2+} cation by a heteroleptic helicate composed from ligands containing bipyridine and terpyridine units.[8] Double-stranded metal helicates were also shown to bind and inhibit DNA cleavage by restriction enzymes.[12] Lehn's group has recently reported on some very remarkable molecular structures comprising helicates.[13,14] To date, most of the trinuclear double-stranded helicates and larger helicates were prepared with copper cations.

The new ligand 2,9-bis[(6-methyl-2,2′-bipyridin-6′-yl)-methyleneoxymethylen-yl]-1,10-phenanthroline (**1**) and its double-stranded zinc(II), copper(I) and silver(I) helicates were prepared. These helicates, which have the general formula $[(\mathbf{1})_2M_3]^{3n+}$ ($n = 1$ for Cu^+ and Ag^+ and $n = 2$ for Zn^{2+}), were characterized by 1D, 2D and diffusion NMR. The silver and the copper helicates were also characterized by FAB mass spectrometry. For $[(\mathbf{1})_2Cu_3]^{3+}$ we obtained the crystal structure. The dynamic behavior of the copper and the silver helicates in solution is reported, along with a comparison between the ^1H NMR spectrum and the crystal structure of $[(\mathbf{1})_2Cu_3]^{3+}$ and related copper helicates such as 6″,6‴-bis[(6-methyl-2,2′-bipyridin-6′-yl)methyleneoxymethylen-yl]-2″,2‴-bipyridine (**2**),[3a] 1,2-bis(6-methyl-2,2′-bipyridin-6′-yl)-ethane (**3**) and 1,2-bis(9-methyl-1,10-phenanthrolin-2-yl)-ethane (**4**) (Scheme 1).[15]

Results and discussion

Synthesis of ligand and complexes

Ligand **1** was prepared by reacting 1 equiv. of the dilithium salt of 2,9-bis(hydroxymethyl)-1,10-phenanthroline (**5**) with 2 equiv. of 6-bromomethyl-6′-methyl-2,2′-bipyridine (**6**) in dry THF (Scheme 2).[3a] Compounds **5** and **6** were prepared according to the literature.[3a,16,17]

Addition of 3 equiv. of $AgCF_3SO_3$ or $Cu(CH_3CN)_4PF_6$ to solutions of 2 equiv. of **1** resulted in an immediate coloring of the solution (pale yellow for the Ag^+ and red for the Cu^+), which was accompanied by a complete change in the ^1H and ^{13}C NMR spectra. It is important to note that in both cases only one species is obtained as concluded from the 500 MHz ^1H NMR spectra of the reaction mixture when the reaction was performed in CD_3CN. The complexes were obtained in nearly quantitative yields, although the isolated yields were lower as the reactions were carried out on a small scale (40–50 mg).

The zinc helicate was obtained by adding 2 equiv. of **1** in methylene chloride to 3 equiv. of $Zn(BF_4)_2$ in methanol. In this case the reaction was slow and a white precipitate

---

† *Non-SI units employed*: 1 kcal ≈ 4.18 kJ; 1 bar = 10^5 Pa.

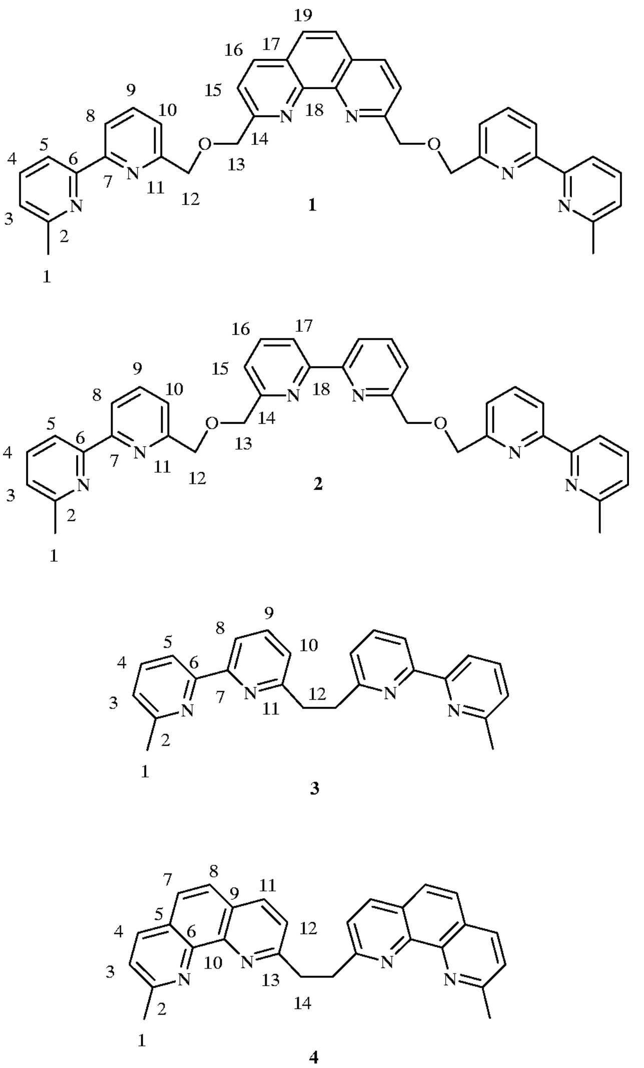

Scheme 1

appeared gradually. After reacting for one week the zinc helicate was obtained in 30% yield.

Helicate characteristics in solution

The ^1H NMR spectra of **1** and its silver, copper and zinc complexes are shown in Fig. 1(*a*), 1(*b*), 1(*c*) and 1(*d*), respectively. These spectra demonstrate that upon complex formation there is a change in the chemical shifts of all peaks. The upfield shift of the peaks attributed to the bridging methylene protons is accompanied also by a change in their hyperfine structure. In the ligand the two methylene protons are equivalent, giving rise to a sharp singlet, while in the double-stranded complexes they are rendered diastereotopic. Consequently, the ^1H NMR signals of these protons change from singlets to AB systems. This is in agreement with the ^1H spectrum of the double-stranded copper and silver helicates of **2**.[3a,c,f] The complete assignments of the ^1H spectra of **1** and its Ag^+, Cu^+ and Zn^{2+} complexes were achieved by long-range 2D COSY experiments as demonstrated for $[(\mathbf{1})_2Ag_3]^{3+}$ (Fig. 2). The cross peaks between the methyl and the methylene protons and the corresponding aromatic protons enable unequivocal assignments of all the protons in the ^1H NMR spectra of these helicates. Once this had been achieved the assignment of all the protonated carbons was carried out by the heteronuclear multiple quantum coherence (HMQC) NMR experiment.[18] The spectral parameters of **1**, $[(\mathbf{1})_2Ag_3]^{3+}$, $[(\mathbf{1})_2Cu_3]^{3+}$, $[(\mathbf{1})_2Zn_3]^{6+}$ and $[(\mathbf{2})_2Cu_3]^{3+}$ as obtained from these experiments are given in the Experimental section. Please note that $[(\mathbf{1})_2Zn_3]^{6+}$ could only be characterized in CD_3CN and not in DMSO-d_6 as the other helicates of **1**.

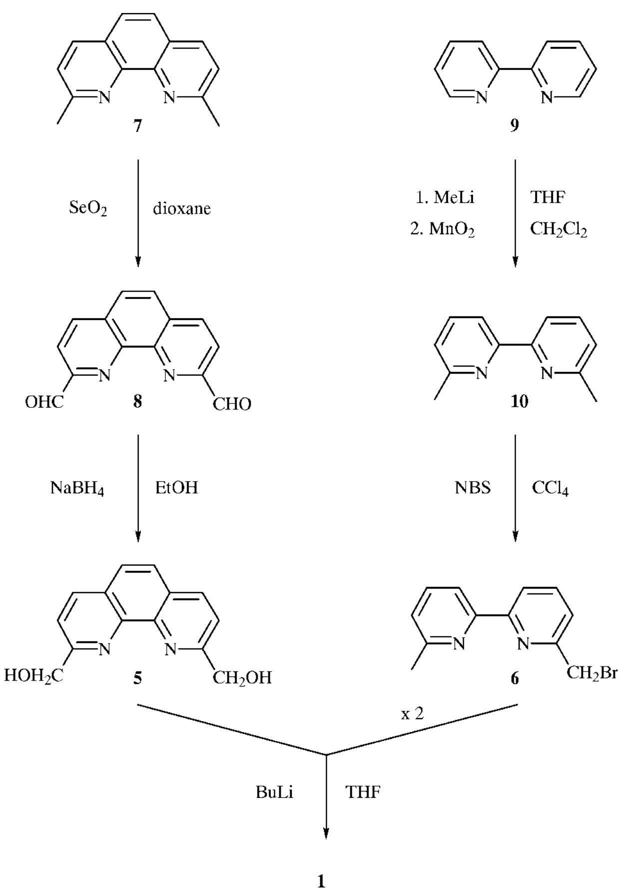

Scheme 2

A peculiar characteristic of the ^1H NMR of the helicates of **1** is the upfield chemical shift of the peak attributed to H-10 (Scheme 1, Fig. 1). Interestingly, this high-field shift, which was found for all d^{10} metal helicates of **1**, was not observed in the copper and silver helicates of **2**.[3a] Even in the copper helicates of **3** and **4** such a high-field shift was not observed.[15] The more meaningful parameter for comparison is not the absolute chemical shift of the protons of these helicates (δ^1H), but rather the change in the chemical shift of each proton upon helicate formation, that is $\Delta\delta^1H$. These values for systems **1**–**4** are summarized in Table 1. These data show that in systems **2**,

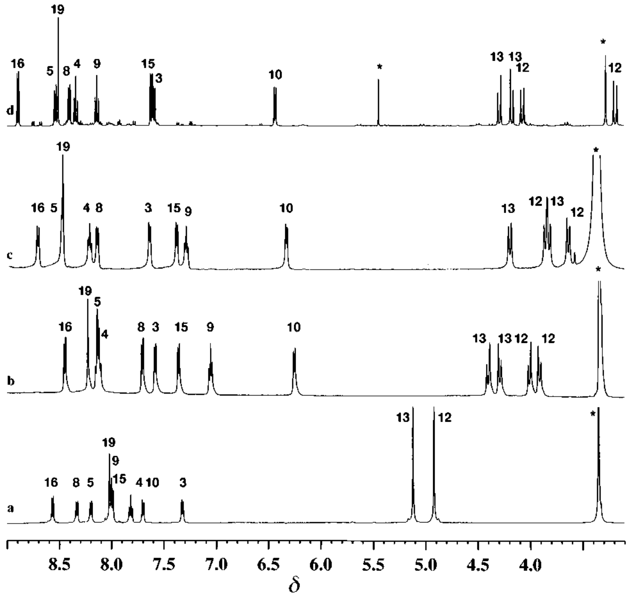

Fig. 1 500 MHz ^1H NMR spectra in DMSO-d_6 at 25 °C of (*a*) **1**, (*b*) $[(\mathbf{1})_2Ag_3]^{3+}$, (*c*) $[(\mathbf{1})_2Cu_3]^{3+}$ and of (*d*) $[(\mathbf{1})_2Zn_3]^{6+}$ in CD_3CN. The asterisks (*) indicate residual water and solvent peaks.

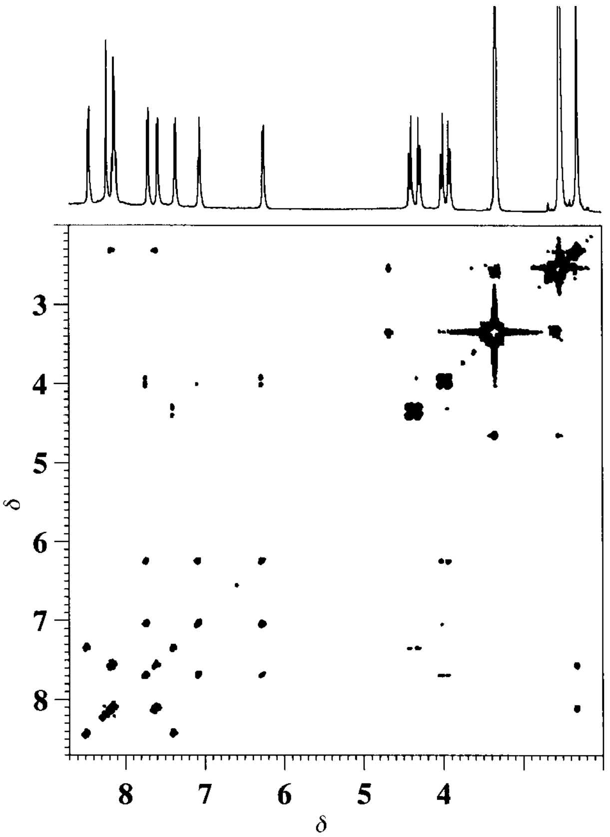

Fig. 2 500 MHz ^1H long-range 2D COSY of $[(\mathbf{1})_2Ag_3]^{3+}$ in DMSO-d_6 at 25 °C.

3 and 4 the $\Delta\delta^1H$ of H-10, H-9, H-12 is +0.68, −0.34 and +0.74, respectively, while $\Delta\delta^1H$ of H-10 for the silver and the copper helicates of **1** are +1.43 and +1.37, respectively. The two related copper helicates $[(\mathbf{1})_2Cu_3]^{3+}$ and $[(\mathbf{2})_2Cu_3]^{3+}$ differ much in the magnitude of the changes in the chemical shifts. These observations clearly indicate that in $[(\mathbf{1})_2M_3]^{3+}$ the inner pyridine rings of the bipyridine units are strongly affected by the shielding effect of the central phenanthroline units while in $[(\mathbf{2})_2Cu_3]^{3+}$ a weaker shielding effect is observed due to the central bipyridine unit. The above observations may also suggest a shorter average distance and a different relative orientation between the central units and the external bipyridine units in $[(\mathbf{1})_2Cu_3]^{3+}$ and $[(\mathbf{2})_2Cu_3]^{3+}$ in solution. Although in system **3** $\Delta\delta^1H$ for H-9 and H-10 are negative, for system **4** the values of H-11 and H-12 are positive but smaller than those recorded for **1**. Therefore, it seems that the different behavior of systems **1** and **2** should be attributed to a superposition of the above effects. We have obtained also the crystal structure for $[(\mathbf{1})_2Cu_3]^{3+}$; however, it is difficult to rely on this, since it is clear that the average solution structure of $[(\mathbf{1})_2Cu_3]^{3+}$ is somewhat different from its structure in the solid state (*vide infra*).

The formation of trinuclear double-stranded copper and silver helicates of **1** is supported by the FAB-MS. Although it is known that elecrospray mass spectrometry (ES-MS) is superior for characterizing such complexes,[2e] we observed for both the copper and the silver helicates of **1** isolated peaks with *m*/*z* of 1689 and 1829, corresponding to $[(\mathbf{1})_2Cu_3(PF_6)_2]^+$ and $[(\mathbf{1})_2Ag_3(CF_3SO_3)_2]^+$, respectively. FAB-MS experiments performed on the zinc complex of **1** failed to corroborate the formation of a double-stranded complex of the $[(\mathbf{1})_2Zn_3]^{6+}$ type. Therefore, we decided to perform a series of NMR diffusion measurements to probe the double-stranded nature of the zinc complex of **1**. First, we measured the diffusion coefficients of **1** and $[(\mathbf{1})_2Cu_3(PF_6)_3]$ in $CDCl_3$–DMSO-d_6 solution using the pulsed gradient spin echo (PGSE) technique;[19] these were found to be $(0.28 \pm 0.01) \times 10^{-5}$ and $(0.19 \pm 0.01) \times 10^{-5}$ cm^2 s^{-1}, respectively. Assuming only a molecular weight effect on the diffusion coefficients one would expect these values to be inversely proportional to the cubic root of the molecular weights.[20] So, a ratio of 0.69 is expected between the diffusion coefficients of $(\mathbf{1})_2Cu_3(PF_6)_3$ and **1**. The ratio found experimentally (0.68) is very close to this expected value. Once the fact that molecular weight is the dominant factor affecting the diffusion coefficients of these species is established, we compared the diffusion coefficient of the zinc complex of **1** with the diffusion coefficient of $(\mathbf{2})_2Cu_3(PF_6)_3$ under identical conditions with TMS as an internal standard. Fig. 3 shows the decay of the natural log of the normalized signal intensity (ln

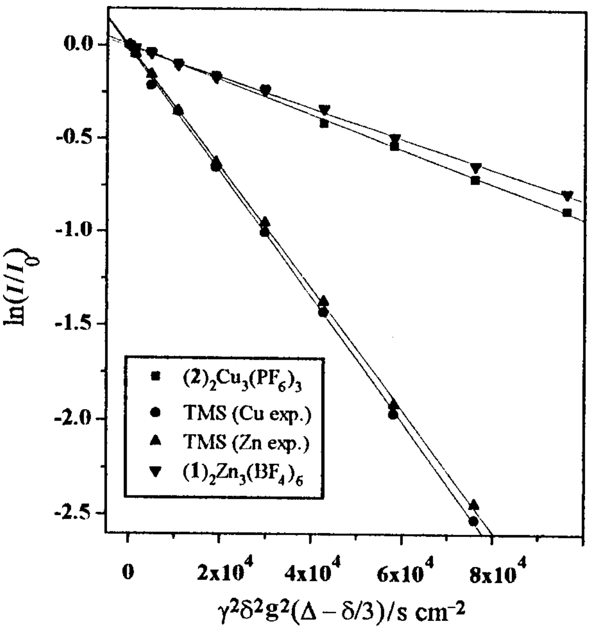

Fig. 3 The decay of the natural log of the normalized echo intensities (ln I/I_0) of the methyl signals of $[(\mathbf{1})_2Zn_3]^{6+}$ and $[(\mathbf{2})_2Cu_3]^{3+}$ and of the TMS signal in both experiments as a function of pulsed gradient strength. Note that (ln I/I_0) is plotted against $\gamma^2\delta^2g^2(\Delta - \delta/3)$.

Table 1 ^1H NMR chemical shift changes ($\Delta\delta$ ^1H) upon formation of the copper helicates of **1**, **2**, **3** and **4**.[a]

	Position															
System	1	3	4	5	7	8	9	10	11	12, 12′	13, 13′	14	15	16	17	19
1[b]	+0.49	−0.32	−0.39	−0.30		+0.19	+0.72	+1.37		+1.06, +1.28	+0.92, +1.30		+0.62	−0.14		−0.48
2[b]	+0.46	−0.29	−0.34	−0.27		−0.15	−0.06	+0.68[d]		+1.0, +1.3	+1.0, +1.3		+0.84[d]	+0.17	−0.04	
3[c]	+0.58	−0.30[d]	−0.34[d]	+0.20[d]		+0.20[d]	−0.34[d]	−0.30[d]		+0.45						
4[c]	+0.57	−0.10	−0.41		−0.38	−0.12			+0.56	+0.74		+0.86				

[a] (−) and (+) represent downfield and upfield shifts, respectively, upon helicate formation. Numbering according to Scheme 1. [b] Data from the present study (spectra of both ligands and their helicates were taken in DMSO-d_6). [c] Data taken from ref. 15 and ref. 8 cited therein (ligand chemical shifts were taken in CD_2Cl_2; helicate chemical shifts were taken in CD_3CN). [d] Where proton assignment is not certain the maximal shift observed is presented.

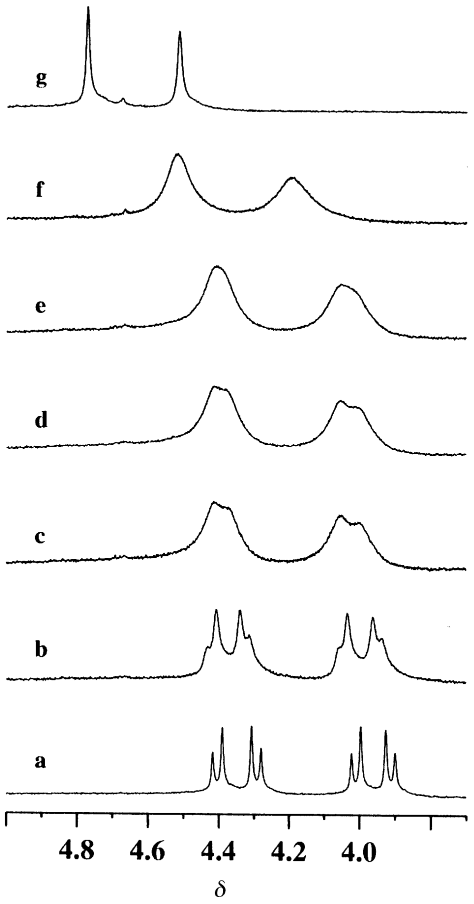

Fig. 4 500 MHz ^1H VT-NMR spectra in DMSO-d_6 of the protons of the CH_2OCH_2 bridges of $[(\mathbf{1})_2Ag_3]^{3+}$ at (*a*) 22, (*b*) 43, (*c*) 57, (*d*) 60, (*e*) 62, (*f*) 102 and (*g*) 158 °C.

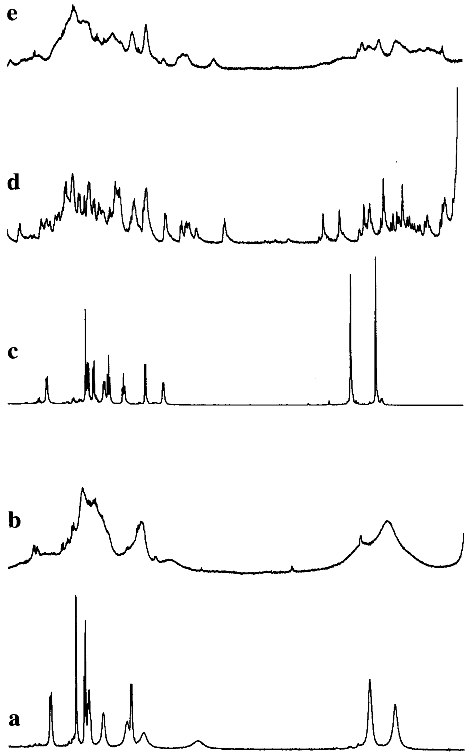

Fig. 5 500 MHz ^1H NMR spectra in DMSO-d_6 of (*a*) $[(\mathbf{1})_2Ag_3]^{3+}$ at ≈90 °C, (*b*) a mixture of **1** and $[(\mathbf{1})_2Ag_3]^{3+}$ at 25 °C, (*c*) a mixture of **1** and $[(\mathbf{1})_2Ag_3]^{3+}$ at ≈90 °C, (*d*) a mixture of **1** and $[(\mathbf{1})_2Cu_3]^{3+}$ at 25 °C and (*e*) a mixture of **1** and $[(\mathbf{1})_2Cu_3]^{3+}$ at ≈90 °C.

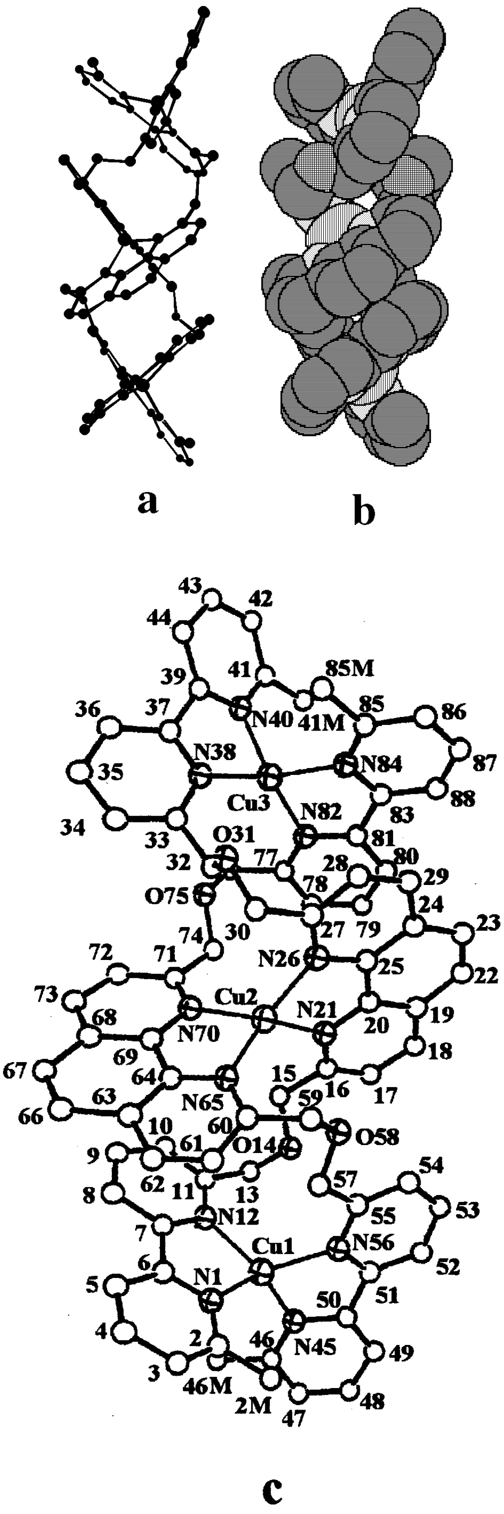

Fig. 6 The crystal structure of $[(\mathbf{1})_2Cu_3(PF_6)_3]$: (*a*) a side view, (*b*) a space-filling model based on the crystallographic data and (*c*) an ORTEP representation where the atoms are shown as 30% thermal spheres. For clarity all drawings omit both the hydrogens and the PF_6^- anions.

I/I_0) of the methyl peaks of $(\mathbf{2})_2Cu_3(PF_6)_3$ and $(\mathbf{1})_2Zn_3(BF_4)_6$ and that of TMS as a function of the pulse gradient strength. From this graph we calculated the diffusion coefficients of these compounds to be $(0.85 \pm 0.01) \times 10^{-5}$, $(0.81 \pm 0.01) \times 10^{-5}$, $(3.26 \pm 0.03) \times 10^{-5}$ and $(3.21 \pm 0.03) \times 10^{-5}$ $cm^2\ s^{-1}$, respectively. The fact that the diffusion coefficient of the zinc complex of **1** is very similar to and even somewhat lower than the diffusion coefficient of the double-stranded copper helicate of **2** suggests that the molecular weight of the zinc complex of **1** should be at least that of $(\mathbf{2})_2Cu_3(PF_6)_3$. Based on the diffusion results and on the similarities in the ^1H NMR spectral characteristics of the copper and the silver helicates of **1** with that of its zinc complex we concluded that the zinc complex is also a double-stranded helicate of the $(\mathbf{1})_2Zn_3(BF_4)_6$ type. To the best of our knowledge $(\mathbf{1})_2Zn_3(BF_4)_6$ is the first trinuclear double-stranded zinc helicate ever prepared.[21]

Fig. 4 shows the ^1H VT-NMR spectra of the protons of the $CH_2{-}O{-}CH_2$ bridges of $[(\mathbf{1})_2Ag_3]^{3+}$. From this figure it seems that the dissociation process of the double-stranded silver helicate occurs in two nearly separate stages. First, there is an enantiomerization/unfolding process in which the helicity of the helicate changes frequently on the NMR time scale, but then at higher temperature there is a dissociation process. The first stage consists of partial unfolding involving reorganization around the metal centers and the second consists of a dissociation of the double-stranded helix into its components. In the first stage of the process there is a collapse of the AB systems into singlets with relatively small changes in their chemical shifts. Then these broad singlets start to sharpen and to move to low field, affording at temperatures higher than 158 °C a ^1H NMR spectrum that resembles that of the free ligand **1**. These changes are in line with the dissociation of the silver helicate to its components. From the coalescence temperatures (T_c, 335 K) a free energy of activation ($\Delta G^{\#}{}_{335}$) of 16.6 ± 0.2 kcal mol^{-1} was calculated for the first process of $[(\mathbf{1})_2Ag_3]^{3+}$ in DMSO-d$_6$.[22] The lability of the silver helicate is further exemplified in Fig. 5, which demonstrates that addition of free ligand to its DMSO solution, even at 25 °C, results in a dramatic broadening of the spectrum [Fig. 5(*b*)]. Further heating of this mixture to ≈90 °C resulted in a sharpening of the spectrum [Fig. 5(*c*)]. At this temperature it seems that the partially dissociated helicate and the free ligand **1** are in fast exchange on the NMR time scale, affording a spectrum that is very similar to that of the free ligand **1**. It should be noted that all these spectral changes are reversible and cooling regenerated the original starting spectra [Fig. 5(*b*) and 1(*b*)]. When the same experiments were performed on the copper helicate of **1** it was found that heating the solution of $[(\mathbf{1})_2Cu_3]^{3+}$ to ≈90 °C had no effect on the ^1H NMR spectrum. Addition of **1** to a solution of $[(\mathbf{1})_2Cu_3]^{3+}$ at 25 °C afforded a complicated spectrum that seems to be a superposition of the spectra of **1**, $[(\mathbf{1})_2Cu_3]^{3+}$ and additional species [see Fig. 5(*d*)]. Fig. 5(*d*) demonstrates that these species are in slow exchange on the NMR time scale at this temperature under these conditions. Heating the mixture of **1** and $[(\mathbf{1})_2Cu_3]^{3+}$ to ≈90 °C results in a broadening of the NMR spectrum due to an increase in the exchange rate between the different species [Fig. 5(*e*)]. All these results are consistent with the fact that the silver helicate is more labile than the copper helicate of **1**.

Solid state structure

The crystal structure of the copper complex of **1**, shown in Fig. 6, confirms its double-helical structure. Table 2 gives selected bond lengths, bond angles and distances in $[(\mathbf{1})_2Cu_3, (PF_6)_3]$. It should be noted that although the NMR data at room temperature is consistent with a double-stranded complex having an average D_2 symmetry in solution, the crystal structure shows that this is not the case in the solid

Table 2 Selected bond lengths (Å), distances (Å), and bond angles (deg) for $(\mathbf{1})_2Cu_3(PF_6)_3$[a]

Cu1—N1	2.033(9)	Cu3—N84	2.004(9)	C25—N26	1.362(13)
Cu1—N12	2.026(9)	N1—C2	1.340(15)	N26—C27	1.326(11)
Cu1—N45	2.051(8)	N1—C6	1.332(15)	C33—N38	1.350(14)
Cu1—N56	2.013(9)	C7—N12	1.345(14)	C37—N38	1.355(15)
Cu2—N21	2.051(9)	C11—N12	1.338(13)	C39—N40	1.366(15)
Cu2—N26	2.032(7)	N40—C41	1.343(16)	C64—N65	1.368(15)
Cu2—N65	2.029(8)	N45—C46	1.336(15)	C69—N70	1.376(13)
Cu2—N70	2.036(9)	N45—C50	1.344(17)	N70—C71	1.331(15)
Cu3—N38	2.028(9)	C51—N56	1.345(14)	C77—N82	1.320(12)
Cu3—N40	2.021(10)	C55—N56	1.351(14)	C81—N82	1.325(15)
Cu3—N82	2.030(9)	C60—N65	1.329(15)	N84—C85	1.344(13)
C16—N21	1.299(11)	C83—N84	1.356(16)	C20—N21	1.384(12)
N45—Cu1—N56	81.6(4)	N21—Cu2—N70	121.1(3)		
N12—Cu1—N56	131.9(3)	N21—Cu2—N65	127.9(3)		
N12—Cu1—N45	124.3(3)	N21—Cu2—N26	82.6(3)		
N1—Cu1—N56	129.4(4)	N82—Cu3—N84	81.4(4)		
N1—Cu1—N45	113.2(4)	N40—Cu3—N84	123.5(4)		
N1—Cu1—N12	80.8(3)	N40—Cu3—N82	127.8(4)		
N65—Cu2—N70	82.8(3)	N38—Cu3—N84	124.8(4)		
N26—Cu2—N70	126.9(3)	N38—Cu3—N82	124.0(4)		
N26—Cu2—N65	121.5(3)	N38—Cu3—N40	81.6(3)		
C5—C6—C7—C8	0.8	N38—C37—C39—N40	17.4		
C19—C20—C25—C24	−0.3	N45—C50—C51—N56	23.4		
C36—C37—C39—C44	15.0	N65—C64—C69—N70	0		
C49—C50—C51—C52	27.9	N82—C81—C83—N84	0.9		
C63—C64—C69—C68	1.7	C11—C13—C15—C16	142.9		
C80—C81—C83—C88	−5.9	C27—C30—C32—C33	157.3		
N1—C6—C7—N12	5.0	C55—C57—C59—C60	−132.8		
N21—C20—C25—N26	2.5	C71—C74—C76—C77	146.5		
Metal–metal distances and angle					
Cu1 ··· Cu2	5.989	Cu2 ··· Cu3	6.236	Cu1 ··· Cu3	12.009
		Cu1 ··· Cu2 ··· Cu3	158.4		
Edge-to-edge distances					
C2M ··· C41M	16.84	C46M ··· C41M	16.84		
C2M ··· C85M	15.60	C46M ··· C85M	16.84		

[a] For numbering of atoms see Fig. 6(*c*).

state. Here the two strands of the helicate are similar but not identical. The distances between Cu1 and Cu2 and between Cu2 and Cu3 were found to be 5.989 and 6.236 Å, respectively. The three copper ions are not collinear and the distance between Cu1 and Cu3 is 12.009 Å with the Cu1···Cu2···Cu3 angle being 158.4°. It should be noted that such a non-collinearity between the three copper atoms was observed in the copper helicate of **2**, though the exact angle was not reported.[3a] This means that in solution a fast dynamical process of bending and twisting must occur in order to obtain an averaged structure on the NMR time scale that has a D_2 symmetry.

The average Cu—N bond length (2.02 ± 0.03 Å) is very similar to that observed for $[(\mathbf{2})_2Cu_3]^{3+}$ and for the bis(6,6′-dimethyl-2,2′-bipyridine)·Cu^+ complex.[3a,23] The N—Cu—N bond angles for Cu1 differ from those observed for Cu2 and Cu3 (Table 2). For Cu1, of the six angles two are around 81° and four are in the range of 113–132° while for Cu2 and Cu3 two angles are around 81° and the other four are in the range of 121–128°. Interestingly, from the crystal structure it can be seen that only one of the two bipyridine units of each strand has a large dihedral angle between its two pyridine units. Although these values for $[(\mathbf{2})_2Cu_3]^{3+}$ were not reported, the crystal structure of $[(\mathbf{2})_2Ag_3]^{3+}$ shows that two of the three bipyridine units of each strand have a significant dihedral angle between their pyridine rings, larger than 10°. Since such a dihedral angle is not possible for the central phenanthroline unit one could anticipate that the total length, or more precisely the pitch length, will be longer in $[(\mathbf{1})_2Cu_3]^{3+}$ than in $[(\mathbf{2})_2Cu_3]^{3+}$. However, it seems that the total length and pitch length of $[(\mathbf{1})_2Cu_3]^{3+}$, which are around ≈17 Å and 12–13 Å (Table 2), respectively, are similar to those reported[3a] for $[(\mathbf{2})_2Cu_3]^{3+}$.

Experimental

General

^1H and ^{13}C NMR spectra were recorded either on a AC 200 or on a ARX 500 Bruker spectrometer (Karlsruhe, Germany). NMR spectra of the ligands and their respective complexes, as well as the NMR diffusion measurements, were all recorded on the ARX 500 NMR spectrometer using an inverse probe equipped with a self-shielded *z*-gradient coil. The gradients were driven by a B-AFPA 10 unit capable of producing *z*-gradients of up to 50 G cm^{-1}. All chemical shifts are reported in ppm measured relative to residual protonated solvents (δ DMSO-d_6 2.53, δ CD_3CN 1.93 and δ $CDCl_3$ 7.26). ^{13}C chemical shifts are also reported in ppm relative to the ^{13}C solvent resonances (δ DMSO-d_6 39.5, δ $CDCl_3$ 77.0 and δ CD_3CN 117.2) and the spin-spin couplings are reported in hertz. ^1H VT-NMR spectra were acquired on the 500 ARX spectrometer.

The diffusion coefficients of **1** and $[(\mathbf{1})_2Cu_3](PF_6)_3$ were measured in a 1:1 solution of DMSO-d_6–$CDCl_3$ (v/v) with TMS used as an internal reference while the diffusion coefficients of $[(\mathbf{1})_2Cu_3](PF_6)_3$ and $[(\mathbf{1})_2Zn_3](BF_4)_6$ were measured in CD_3CN. All diffusion measurements were performed at 25 °C and the parameters used in the PGSE experiments were as published previously.[24] The $\Delta G^{\#}$ values were calculated from the coalescence temperature (T_c) according to ref. 25(*a*). The temperature was estimated from the changes in the ^1H NMR spectra of ethylene glycol according to ref. 25(*b*).

Fast atomic bombardment mass spectra (FAB-MS) were recorded on a VG-AutoSpec M250 mass spectrometer (Manchester, UK) in a *m*-nitrobenzyl alcohol (NBA) matrix. X-Ray diffraction data were collected using a CAD4 diffractometer. UV-visible spectra were recorded on a Kontron UVIKON 931 UV-vis spectrometer (Zurich, Switzerland). THF was dried over sodium wire under an inert atmosphere.

Synthesis

2,9-Bis[(6-methyl-2,2′-bipyridin-6′-yl)methylenoxymethylenyl]-1,10-phenanthroline (1). Compound $\mathbf{5}^{17}$ (364 mg, 1.5 mmol) was dissolved in dry THF (30 cm^3) under an inert atmosphere and cooled to −70 °C. Butyllithium 1.6 M (2.1 cm^3, 3.3 mmol) was added dropwise to the stirred solution of **5** while keeping the temperature between −70 and −60 °C. The colored reaction mixture was stirred for an additional 1/2 h and then allowed to reach room temperature. At this point compound $\mathbf{6}^{26}$ (837 mg, 3.2 mmol) was added in one portion and the reaction mixture was refluxed for 5 days. The crude product was filtered and washed with THF (≈20 cm^3) and then transferred to a flask containing 30 cm^3 of chloroform and heated for 20 min (55–60 °C). The sticky solids obtained after filtration were dissolved in 5 cm^3 of methanol from which ligand **1** precipitated. After drying (≈50 °C, 20 mbar), 130 mg of a white powder of **1** were obtained. Evaporation of the filtrates followed by recrystallization from methanol or chromatography [alumina, dichloromethane–MeOH (100:0 to 99:1)] gave an additional 183 mg of white powder having a mp of 103 °C (total yield ≈34%). ^1H NMR (500 MHz, DMSO-d_6): 8.56 (d, 8.5, H-16, 2H), 8.33 (d, 7.6, H-8, 2H), 8.20 (d, 7.7, H-5, 2H), 8.02, 8.01, 8.00 (s, t, d, 7.5, 8.5, H-19, H-9, H-15, 6H), 7.82 (t, 7.7, H-4, 2H), 7.70 (d, 7.6, H-10, 2H), 7.32 (d, 7.7, H-3, 2H), 5.12 (s, H-13, 4H), 4.92 (s, H-12, 4H), 2.59 (s, H-1, 6H). ^{13}C NMR (125 MHz, DMSO-d_6): 158.5, 157.6, 157.5, 154.8, 154.4, 144.6, 137.8 (C-9), 137.3 (C-4), 137.0 (C-16), 127.8, 126.2 (C-19), 123.5 (C-3), 121.7 (C-10), 121.0 (C-15), 119.2 (C-8), 117.6 (C-5), 73.7 (C-13), 73.4 (C-12), 24.2 (C-1). UV (CH_3CN): 198, 233, 272, 282 nm. FAB-MS: (DMSO, NBA): *m*/*z* 649 ($\mathbf{1}\cdot K^+$, 1.7%), 627 ($\mathbf{1}\cdot Na^+$, 6%), 611 ($\mathbf{1}\cdot Li^+$, 14%), 605 ($\mathbf{1}\cdot H^+$, 23%).

6″,6‴-Bis[(6-methyl-2,2′-bipyridin-6′-yl)methyleneoxymethylen-yl]-2″,2‴-bipyridine (2)

Compound **2**, known also as BP_3, was prepared according to the literature[3a] and gave the expected ^1H NMR spectrum. ^1H NMR (500 MHz, CD_2Cl_2): 8.32 (d, 7.7, H-8, H-17, 4H), 8.19 (d, 7.7, H-5, 2H), 7.83 (t, 7.7, H-9, H-16, 4H), 7.68 (t, 7.7, H-4, 2H), 7.54 (d, 7.7, H-10 or H-15, 2H), 7.52 (d, 7.7, H-10 or H-15, 2H), 7.16 (d, 7.7, H-3, 2H), 4.85 (s, H-12, H-13, 8H), 2.58 (s, H-1, 6H).

$[(\mathbf{1})_2Ag_3](CF_3SO_3)_3$. A solution of $AgCF_3SO_3$ (45 mg, 0.175 mmol, 2 equiv.) in acetonitrile (2 cm^3) was added to a suspension of **1** (52 mg, 0.086 mmol) in acetonitrile (1 cm^3). The yellow solution obtained was stirred over night. The solution of the complex was then filtered over Celite through a Pasteur pipette. Diethyl ether was added until the complex precipitated completely. The solvent was removed by decantation and the product was washed successively with diethyl ether–dichloromethane solution (9:1), diethyl ether–acetonitrile solution (95:5) and then by diethyl ether. Finally the product was dried (50 °C, 25 mbar) giving 49 mg of beige powder (yield 58%). ^1H NMR (500 MHz, DMSO-d_6): 8.45 (d, 8.2, H-16, 4H), 8.23 (s, H-19, 4H), 8.13 (m, H-5, H-4, 8H), 7.71 (d, 7.8, H-8, 4H), 7.59 (d, 7.6, H-3, 4H), 7.36 (d, 8.2, H-15, 4H), 7.06 (t, 7.8, H-9, 4H), 6.25 (d, 7.8, H-10, 4H), 4.40–4.29 (AB, 13.7, H-13, 8H), 4.01–3.91 (AB, 12.9, H-12, 8H), 2.31 (s, H-1, 12H). ^{13}C NMR (125 MHz, DMSO-d_6): 157.6, 155.8, 155.0, 149.9, 149.6, 140.1, 139.4 (C-4), 138.5(C-16), 138.1 (C-9), 128.1, 127.0 (C-19), 125.4 (C-3), 122.5 (C-10), 122.0 (C-15), 120.8 (C-8), 120.2 (C-5), 72.2 (C-13), 71.8 (C-12), 25.9 (C-1). UV-vis (CH_3CN): 195, 234, 278, 298 nm. FAB-MS (DMSO, NBA): *m*/*z* 1829 ($[(\mathbf{1})_2Ag_3(CF_3SO_3)_2]^+$, 1.7%), 968 ($[\mathbf{1}\cdot Ag_2CF_3SO_3]^+$, 17%), 713 ($\mathbf{1}\cdot Ag^+$, 100%).

$[(\mathbf{1})_2Cu_3](PF_6)_3$. A solution of $Cu(CH_3CN)_4PF_6$ (46 mg, 0.123 mmol, 1.5 equiv.) in acetonitrile (2 cm^3) was added to a suspension of **1** (50 mg, 0.083 mmol) in acetonitrile (1 cm^3). The red solution obtained was stirred over night. The solution was filtered over Celite through a Pasteur pipette and concentrated by evaporation. Diethyl ether was added until the complex precipitated completely. The solvent was removed by decantation and the product was washed as previously. Finally, the product was filtered and dried (50 °C, 25 mbar) affording 66 mg of red powder (yield 87%). It was recrystallized from an acetonitrile solution by slow diffusion of diethyl ether to give fine red needles having a mp of 252 °C (285 °C dec.). These crystals were found to be suitable for X-ray crystallography. ^{1}H NMR (500 MHz, DMSO-d$_6$): 8.70 (d, 8.1, H-16, 4H), 8.50 (d, 7.7, H-5, 4H), 8.50 (s, H-19, 4H), 8.21 (t, 7.7, H-4, 4H), 8.14 (d, 7.7, H-8, 4H), 7.64 (d, 7.7, H-3, 4H), 7.38 (d, 8.1, H-15, 4H), 7.29 (t, 7.7, H-9, 4H), 6.33 (d, 7.7, H-10, 4H), 4.20–3.82 (AB, 13.4, H-13, 8H), 3.86–3.64 (AB, 13.4, H-12, 8H), 2.10 (s, H-1, 12H). ^{13}C NMR (125 MHz, DMSO-d$_6$): 156.5, 154.9, 154.1, 150.7, 150.0, 141.4, 138.4 (C-4), 137.8 (C-16) , 137.4 (C-9), 128.2, 126.9 (C-19), 126.0 (C-3), 123.4 (C-15), 122.6 (C-10), 120.6 (C-8), 119.8 (C-5), 71.5 (C-13), 70.8 (C-12), 24.6 (C-1). UV-vis (CH_3CN): 194, 230, 288, 299, 452 nm. FAB-MS (DMSO, NBA): *m/z* 1689 ($[(\mathbf{1})_2Cu_3(PF_6)_2]^+$, 10%), 667 ($[\mathbf{1}\cdot Cu]^+$, 100%).

$[(\mathbf{1})_2Zn_3](BF_4)_6$. This helicate was prepared by a modification of the procedure used to prepare the Zn complex of 2,9-dimethyl-1,10-phenanthroline.[21] A solution of $Zn(BF_4)_2$ (19.2 mg, 0.08 mmol) in dichloromethane (2 cm^3) was added to a solution of **1** (30.2 mg, 0.05 mmol) in dichloromethane (2 cm^3). The mixture was stirred for 7 days at room temperature, during which time a white precipitate was formed. The precipitate was washed with a 1 : 1 MeOH–CH_2Cl_2 solution and dried, affording 20 mg of white powder (yield 21%), mp 330 °C. ^{1}H NMR (500 MHz, CD_3CN): 8.89 (d, 8.3, H-16, 2H), 8.54 (d, 8.0, H-5, 4H), 8.51 (s, H-19, 4H), 8.40 (d, 8.1, H-8, 4H), 8.34 (t, 7.9, H-4, 4H), 8.14 (t, 8.0, H-9, 4H), 7.61 (d, 8.3, H-15, 4H), 7.59 (d, 7.8, H-3, 4H), 6.43 (d, 7.8, H-10, 4H), 4.29 (d, 14.1, H-13, 4H), 4.17 (d, 14.1, H-13, 4H), 4.07 (d, 15.3, H-12, 4H), 3.18 (d, 15.4, H-12, 4H), 1.46 (s, H-1, 12H). ^{13}C NMR (125 MHz, CD_3CN): 160.4, 156.0, 156.0, 149.4, 147.1, 145.1 (C-16), 144.5 (C-9), 143.8 (C-4), 139.0, 130.2 (C-15), 129.7 (C-19), 129.4, 127.2 (C-3), 125.3 (C-10), 124.7 (C-8), 122.6 (C-5), 72.1 (C-13), 70.4 (C-12), 22.4 (C-1).

$[(\mathbf{2})_2Cu_3](PF_6)_3$. This helicate was prepared using a procedure similar to that of Lehn *et al.*[3a] with $Cu(CH_3CN)_4PF_6$ and gave the expected ^{1}H and ^{13}C NMR spectra and the expected FAB-MS spectrum. ^{1}H NMR (500 MHz, DMSO-d$_6$): 8.48, 8.47 (d, d, 7.8, H-8, H-5, 8H), 8.37 (d, 7.9, H-17, 4H), 8.18 (t, 7.8, H-4, 4H), 8.07 (t, 7.8, H-9, 4H), 7.84 (t, 7.9, H-16, 4H), 7.63 (d, 7.8, H-3, 4H), 6.97 (d, 7.8, H-10, 4H), 6.81 (d, 7.9, H-15, 4H), 3.94, 3.92 (d, d, 13.4, H-12, H-13, 8H), 3.62, 3.57 (d, d, 13.4, H-13, H-12, 8H), 2.14 (s, H-1, 12H). ^{13}C NMR (125 MHz, DMSO-d$_6$): 156.4, 154.4, 154.3, 150.9, 150.1, 149.9, 138.6 (C-9), 138.3 (C-4, C-16), 125.9 (C-3), 123.6 (C-10), 123.2 (C-15), 121.4, 119.7 (C-5, C-8), 121.1 (C-17), 70.8 (C-12, C-13), 24.6 (C-1). FAB-MS (DMSO, NBA): *m/z* 1639 ($[(\mathbf{2})_2Cu_3(PF_6)_2]^+$, 2.3%), 643 ($[\mathbf{2}\cdot Cu]^+$, 89%).

Crystal structure of $[(\mathbf{1})_2Cu_3](PF_6)_3$ ($C_{76}H_{64}N_{12}O_4Cu_3\cdot 3PF_6$)

Diffraction data were collected using a CAD4 diffractometer equipped with a graphite monochromator at 295 K, using Mo-Kα radiation ($\lambda = 0.7107$ Å). Intensity data were collected in the $\omega - 2\vartheta$ scan mode. Crystal data: triclinic, space group $P\bar{1}$, $a = 10.675(5)$, $b = 19.041(4)$, $c = 19.706(6)$ Å, $\alpha = 98.70(2)$, $\beta = 104.44(3)$, $\gamma = 93.96(3)°$, $U = 3810.4$ Å^3, $Z = 2$, $D_{\mathrm{calc}} = 1.599$ g cm^{-3}, $F(000) = 1860$, μ(Mo-Kα) = 9.96 cm^{-1}, crystal size 0.40 × 0.30 × 0.10 mm. Data collection and refinement: diffraction data measured out to $2\vartheta_{\max} = 42°$ with constant scan rate of 2 deg min^{-1}. A total of 7061 unique reflections with positive intensities were recorded. The structure was solved by direct methods (SHELXS-86)[27] and refined by full-matrix least-squares (SHELXL-93).[28] The final refinement, based on F^2, converged at $R = 0.064$ for 4847 observations having $F_o > 4\sigma(F_o)$ and $R = 0.101$ ($wR_2 = 0.18$) for 7061 unique data. At convergence, $S = 1.01$ and $|\Delta p| < 0.48$ e Å^{-3}. The asymmetric unit of this structure consists of an 85-atom double-stranded helical assembly, half of the PF_6 ions were located on inversion centers at 0,0,0 and at 0,0,1/2, and two PF_6 ions in general positions. One of the latter moieties is rationally disordered about P (structure factor calculations were based on a twofold disordered model of the F atoms with refined occupancies of 0.65 and 0.35 for the two sites). Non-hydrogen atoms were treated anisotropically (with the exception of fluorine atoms of a disordered PF_6 ion, which were refined with anisotropic U). All the hydrogen atoms were located in calculated positions.

CCDC reference number 440/091.

References

1 (*a*) F. Vogtle, *Supramolecular Chemistry*, John Wiley & Sons, Chichester, 1991. (*b*) J.-M. Lehn, *Supramolecular Chemistry, Concepts and Perspectives*, VCH, Weinheim, 1995.

2 (*a*) J.-M. Lehn, *Angew. Chem., Int. Ed. Engl.*, 1990, **29**, 1304. (*b*) J. S. Lindsey, *New J. Chem.*, 1991, **15**, 153. (*c*) J.-M. Lehn, *Science*, 1993, **260**, 1762. (*d*) D. B. Amabilino and J. F. Stoddart, *Chem. Rev.*, 1995, **95**, 2725. (*e*) C. Piguet, G. Bernardinelli and G. Hopfgartner, *Chem. Rev.*, 1997, **97**, 2005.

3 For selected examples of double helical complexes see: (*a*) J.-M. Lehn, A. Rigault, J. Siegel, J. Harrowfield, B. Chevrier and D. Moras, *Proc. Natl. Acad. Sci. USA.*, 1987, **84**, 2565. (*b*) J.-M. Lehn and A. Rigault, *Angew. Chem., Int. Ed. Engl.*, 1988, **27**, 1095. (*c*) T. M. Garrett, U. Koert, J.-M. Lehn, A. Rigault, D. Meyer and J. Fischer, *J. Chem. Soc., Chem. Commun.*, 1990, 557. (*d*) U. Koert, M. M. Harding and J.-M. Lehn, *Nature* (*London*), 1990, **346**, 339. (*e*) B. Schoentjes and J.-M. Lehn, *Helv. Chim. Acta*, 1995, **78**, 1. (*f*) A. Marquis-Rigault, A. Dupont-Gervais, A. Van Dorsselaer and J.-M. Lehn, *Chem. Eur. J.*, 1996, **2**, 1395. (*g*) A. Bilyk and M. M. Harding, *J. Chem. Soc., Dalton Trans.*, 1994, 77.

4 (*a*) E. C. Constable, M. G. B. Drew and M. D. Ward, *J. Chem. Soc., Chem. Commun.*, 1987, 1600. (*b*) E. C. Constable and M. D. Ward, *J. Am. Chem. Soc.*, 1990, **112**, 1256. (*c*) E. C. Constable, *Tetrahedron*, 1992, **48**, 10013 and references cited therein. (*d*) E. C. Constable and J. V. Walker, *J. Chem. Soc., Chem. Commun.*, 1992, 884. (*e*) E. C. Constable, F. R. Heirtzler, M. Neuburger, D. R. Smith and M. Zehnder, *Chem., Commun.*, 1996, 933. (*f*) R. Chotalia, E. C. Constable, M. Neuburger, D. R. Smith and M. Zehnder, *J. Chem. Soc., Dalton Trans.*, 1996, 4207.

5 (*a*) S. Ruttimann, C. Piguet, G. Bernardelli, B. Bocquet and A. F. Williams, *J. Am. Chem. Soc.*, 1992, **114**, 4230. (*b*) K. T. Potts, M. Keshavarz-K, F. S. Tham, H. D. Abruña and C. R. Arana, *Inorg. Chem.*, 1993, **32**, 4422.

6 For selected examples of triple helical complexes see: (*a*) J. Libman, Y. Tor and A. Shanzer, *J. Am. Chem. Soc.*, 1987, **109**, 5880. (*b*) A. F. Williams, C. Piguet and G. Bernardinelli, *Angew. Chem., Int. Ed. Engl.*, 1991, **30**, 1490. (*c*) G. Bernardinelli, C. Piguet and A. F. Williams, *Angew. Chem., Int. Ed. Engl.*, 1992, **31**, 1622. (*d*) R. Kramer, J.-M. Lehn, A. DeCian and J. Fischer, *Angew. Chem., Int. Ed. Engl.*, 1993, **32**, 703. (*e*) C. Piguet, G. Bernardinelli, J.-C. G. Bunzli, S. Petoud and G. Hopfgartner, *J. Chem. Soc., Chem. Commun.*, 1995, 2575.

7 (*a*) L. J. Charbonniere, A. F. Williams, U. Frey, A. E. Merbach, P. Kamalaprija and O. Schaad, *J. Am. Chem. Soc.*, 1997, **119**, 2488. (*b*) C. Piguet, E. Rivera-Minten, G. Bernardinelli, J.-C. G. Bunzli and G. Hopfgartner, *J. Chem. Soc., Dalton Trans.*, 1997, 421.

8 B. Hasenknopf, J.-M. Lehn, G. Baum and D. Fenske, *Proc. Natl. Acad. Sci. USA*, 1996, **93**, 1397.

9 V. C. M. Smith and J.-M. Lehn, *Chem. Commun.*, 1996, 2733.

10 (*a*) E. C. Constable, A. J. Edwards, P. R. Raithby and J. V. Walker, *Angew. Chem., Int. Ed. Engl.*, 1993, **32**, 1465. (*b*) C. Piguet, *Chimia*, 1996, **50**, 144.

11 L. Zelikovich, J. Libman and A. Shanzer, *Nature* (*London*), 1995, **374**, 790.

12 B. Schoentjes and J.-M. Lehn, *Helv. Chim. Acta*, 1995, **78**, 1.

13 B. Hasenkopf, J.-M. Lehn, B. O. Kneisel, G. Baum and D. Fenske, *Angew. Chem., Int. Ed. Engl.*, 1996, **35**, 1838.

14 D. P. Funeriu, J.-M. Lehn, G. Baum and D. Fenske, *Chem. Eur. J.*, 1997, **3**, 99.

15 M.-T. Youinou, R. Ziessel and J.-M. Lehn, *Inorg. Chem.*, 1991, **30**, 2144.

16 C. O. Dietrich-Buchecker, P. A. Marnot and J.-P. Sauvage, *Tetrahedron Lett.*, 1982, **23**, 5291.

17 C. J. Chandler, L. W. Deady and J. A. Reiss, *J. Heterocycl. Chem.*, 1981, **18**, 599.

18 L. Muller, *J. Am. Chem. Soc.*, 1979, **101**, 4481.

19 E. O. Stejskal and J. E. Tanner, *J. Chem. Phys.*, 1965, **42**, 288. For an excellent review concerning the application of the PGSE NMR technique to chemical systems see: P. Stilbs, *Prog. NMR Spectrosc.*, 1987, **19**, 1.

20 A. R. Waldeck, P. W. Kuchel, A. J. Lennon and B. E. Chapman, *Prog. NMR Spectrosc.*, 1997, **30**, 39.

21 Even the simple zinc(II) complex of 2,9-dimethyl-1,10-phenanthroline (**7**), *i.e.* (**7**)$_2$Zn, was prepared only very recently, see: A. J. Pallenberg, T. M. Marschner and D. M. Barnhart, *Polyhedron*, 1997, **16**, 2711.

22 For recent dynamic NMR studies of helicates see: (*a*) R. F. Carina, A. F. Williams and C. Piguet, *Helv. Chim. Acta*, 1988, **81**, 548. (*b*) M. Albrecht, M. Schneider and H. Rottele, *Chem. Ber./Recl.*, 1997, **130**, 615. (*c*) M. Albrecht and M. Schneider, *Chem. Commun.*, 1998, 137. (*d*) B. Kersting, J. R. Telford, M. Meyer and K. N. Raymond, *J. Am. Chem. Soc.*, 1996, **118**, 5712.

23 P. J. Burke, D. R. McMillin and W. R. Robinson, *Inorg. Chem.*, 1980, **19**, 1211.

24 (*a*) O. Mayzel and Y. Cohen, *J. Chem. Soc., Chem. Commun.*, 1994, 1901. (*b*) A. Gafni and Y. Cohen, *J. Org. Chem.*, 1997, **62**, 120.

25 (*a*) H. Gunther, *NMR Spectroscopy: Basic Principles, Concepts and Application in Chemistry*, 2nd edn., John Wiley & Sons, Chichester, 1994, p. 344. (*b*) *ibid.*, p. 66.

26 J.-C. Rodriguez-Ubis, B. Alpha, D. Plancherel and J.-M. Lehn, *Helv. Chim. Acta*, 1984, **67**, 2264.

27 G. M. Sheldrick, *Acta Crystallogr., Sect. A*, 1990, **46**, 467.

28 G. M. Sheldrick, *SHELXL-93, Program for Refinement of Crystal Structures from Diffraction Data*, University of Göttingen, Germany, 1993.

Paper 8/08673G